Development of the in-vehicle pulse sensor

About the pulse rate estimate technique from a microwave sensor

MITANI Shigetomo

In late years accidents due to the health condition of the driver are increasing. The precaution is required all the more.

Therefore we developed the in-vehicle pulse sensor using the microwave sensor. We installed this pulse sensor in the driver's seat and succeeded in even a big state of the disturbance while driving allowing you to estimate the pulse rate of the driver exactly.

We speak effective signal processing algorithm to maintain measurement accuracy as an in-vehicle pulse sensor in this paper.

1. Introduction

In recent years, the development of practical measures to deal with social issues such as anxiety about driving owing to aging and health condition, as well as dangerous driving owing to impaired driving and the use of mobile devices have been desired.

Therefore, the driver monitoring field, where biological information of a driver while driving is obtained to determine the driver's status and provide support appropriate for the status, is attracting attention. In the future, a highly expansive driver monitoring business is expected to be developed by taking unique advantage of an in-vehicle environment where biological information can be obtained for fairly large blocks of time while driving in a limited environment, i.e., the seating position in the cabin, as well as by working with the offering of various services in association with IoT in the future.

Pulse rate is one of the biomarkers for determining a driver's health status. It is considered that pulse rate enables the determination of the driver's stress level.

Therefore, we developed an in-vehicle pulse sensor which enabled accurate estimation of the pulse rate of a driver while driving.

So far, the following types of methods have been considered for a sensor installed on a vehicle seat to measure the driver's pulse rate:

(1) Electrode type (for measuring impedance fluctuation)

(2) Pressure sensor (Piezoelectric element)

(3) Air tube type (Air pressure)

(4) Electrostatic capacitance type

(5) Optical type (utilizing absorption rate fluctuation according to hemoglobin concentration)

(6) Radio wave type

Contact : *MITANI Shigetomo* shigetomo.mitani@omron.com

With any of the above methods, it is relatively easy to estimate the pulse rate as long as a driver is in a resting state in a parked car, but it is very difficult to estimate the pulse rate accurately in the event of significant disturbance while driving. In addition, considering durability, methods (1) – (4) leave issues to be solved. In the case of (5) optical type, the sensor often deviates from the point where the pulse can be measured depending on the seating position, and the frequency of inaccurate measurement increases. The (6) radio wave type has the characteristic of being able to withstand a harsh environment, i.e., in a vehicle, because both relatively stable measurement and contactless measurement are possible. According to previous studies on the radio wave type[1], it was difficult to perform accurate measurement in a vehicle that was actually running in the presence of driving behaviors and extensive processing was required. Therefore, we developed our own signal processing method which can be implemented compactly to enable real-time pulse measurement even while driving.
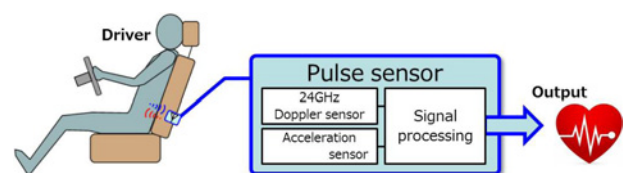

Fig. 1 Conceptual diagram of a radio wave type pulse sensor

As Fig. 1 shows, a pulse sensor is built into the driver's seat and the pulse rate is estimated from the signals detected by a radio wave sensor through digital signal processing. The impacts generated by vehicle vibration are detected and discriminated by the acceleration sensor to prevent inaccurate output of the pulse rate.

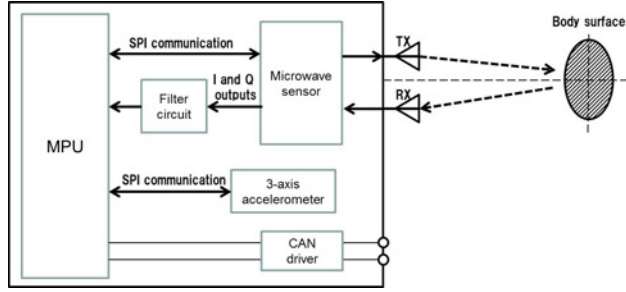## 2. Pulse rate measurement principle

Fig. 2 System configuration of the pulse sensor

Fig. 2 shows the system configuration of the pulse sensor. In the case of a radio wave type pulse sensor, electromagnetic waves (microwave) are radiated from the transmission antenna Tx to the body surface and the reflected waves are received by the receiving antenna Rx. The microwave sensor generates a transmission wave to be transmitted and also outputs I and Q signals after the transmission and receiving waves are mixed. The MPU samples the analog signals of I and Q after passing through the filter using the A/D converter to detect subtle movements on the body surface from the I and Q signals to estimate the pulse rate.

The theoretical formulas of the transmission wave, receiving wave and signal after mixing are expressed by equations $(1)-(3)$, and the theoretical formulas of I and Q output signals are given by equations (4) and (5) which are expressed based on equation (3) by leaving only the term including the Doppler angular velocity of low frequency and delaying the phase of Q output by $\pi/2$ relative to I output.

· Theoretical formula of transmission wave

$$x_s(t) = A_s \cos(\omega_s t) \tag{1}$$

· Theoretical formula of receiving wave

$$x_r(t) = A_r \cos\big([\omega_s + \omega_d]t + \varphi\big) \tag{2}$$

· Theoretical formula after mixing

$$
\begin{aligned}
& x_s(t)x_r(t) \\
& = A_s A_r \cos(\omega_s t)\cos\big([\omega_s + \omega_d]t + \varphi\big) \\
& = A_s A_r/2\big\{\cos(\omega_d t + \varphi) + \cos\big([2\omega_s + \omega_d]t + \varphi\big)\big\}
\end{aligned}
\tag{3}
$$

· Theoretical formula of I output

$$I(t) = A_s A_r/2\cos(\omega_d t + \varphi) \tag{4}$$

· Theoretical formula of Q output

$$Q(t) = A_s A_r/2\cos(\omega_d t + \varphi - \pi/2) \tag{5}$$

t : Time

x_s : Transmission wave

ω_s : Angular Velocity of transmission wave

A_s : Amplitude of transmission wave

x_r : Receiving wave

ω_d : Doppler angular velocity

A_r : Amplitude of receiving wave

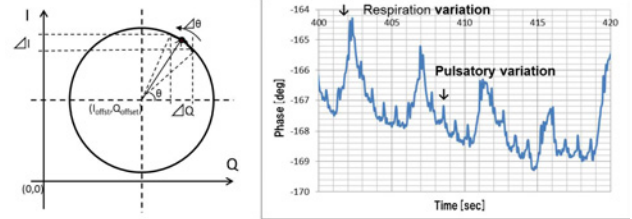φ : The phase depending on the distance from a target

Fig. 3 Observation of body surface with I-Q Lissajous waveform

The movements on the body surface are detected by estimating the Doppler angular velocity ω_d contained in the I and Q outputs. If the phase θ of the I-Q Lissajous waveform formed by the I and Q output signals is defined as shown in the left part of Figure 3 to determine this Doppler angular velocity ω_d, the Doppler angular velocity ω_d is obtained through temporal differentiation of the phase θ. In addition, this phase θ enables the observation of subtle movements on the body surface as shown in the right part of this figure. If the value of the phase θ is converted into displacement, a pulsatory variation as subtle as 10 µm can be observed while the respiratory variation is 50 µm. However, this variation differs depending on the site of measurement and the method of supporting the body surface. In addition, in the non-resting state, it is difficult to observe pulsation because various body movements become a disturbance.

To extract a pulsation signal from being buried in disturbances, this pulse sensor utilizes the digital signal processing method. In addition, using equation (6) as the approximate equation of the Doppler angular velocity ω_d instead of directly calculating the phase θ improved the efficiency of computing and also configured processing that could be implemented in a small microcomputer to successfully achieve downsizing.

· Approximate equation of the Doppler angular velocity ω_d

$$\omega_d \approx \frac{(I - I_{offset}) \times \Delta Q - (Q - Q_{offset}) \times \Delta I}{(I - I_{offset})^2 + (Q - Q_{offset})^2} \tag{6}$$

ΔI : Temporal variation of I output

ΔQ : Temporal variation of Q output

I_{offset} : Central point of the I-Q Lissajous (I axis)

Q_{ffset} : Central point of the I-Q Lissajous (Q axis)

3. Development goal

Fig. 4 External appearance of the pulse sensor

Table 1 Primary specifications of the pulse sensor

Item	Details
Operating temperature	- 20 ◦C – + 70 ◦C
Size	45 × 50 × 17 mm
Consumption current	Max. 150 mA or lower
Communication	C-CAN
Doppler sensor frequency	24.05 – 24.25 GHz
Doppler sensor output intensity	3 dBm
Pulse rate detection range	50 – 160 BPM
Pulse rate estimation accuracy (RMS error)	+/– 10 BPM (while running)

Fig. 4 shows the external appearance of the pulse sensor we developed this time, and Table 1 shows its primary specifications. As Fig. 2 shows, SPI communication sets the registers of the microwave sensor and acceleration sensor for control and also obtains acceleration data from the acceleration sensor. The acceleration data is utilized to detect a disturbance caused by a shock applied to the sensor. The pulse sensor we developed this time can be used in conjunction with an external unit through CAN communication. This configuration achieved downsizing, which made it possible to build the pulse sensor into the seat. In addition, our development goal is to achieve the specifications shown in Table 1 concerning the pulse rate detection range and estimation accuracy.

To clarify the issues with this pulse sensor, the left part of Fig. 5 illustrates the disturbance. If the sensor is built into the driver's seat, the variation in the distance between the body surface and the sensor, as well as the distance between a peripheral metal object and the sensor, could be a major cause. Furthermore, on the body surface, in addition to the pulsation which is subject to observation, respiratory body movement, spontaneous body movement associated with hand, foot and head motions, and impulsive body movement attributable to vehicle vibration while running, could also be the causes of disturbance.

The right part of Fig. 5 shows the variation in the Doppler angular velocity ω_d while running. The disturbance while a

vehicle is running is more than 100 times larger than while it is parked, making it difficult to estimate the pulse rate. To achieve the goal, it is necessary to develop technology to estimate the pulse rate while diminishing the influence of vehicle vibration and spontaneous body movement such as respiration.
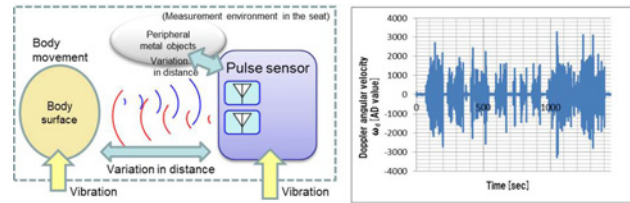

Fig. 5 Disturbance in the in-vehicle pulse sensor

4. Technical content

This chapter describes the contents of the following three major technologies which were developed to solve the above issues:

(1) Correction of the offset misalignment of I-Q Lissajous associated with the change in positional relationship with a peripheral metal object

(2) Synchronous detection for detecting a pulsation period signal buried in disturbance

(3) Removal of periodic artifacts such as respiratory harmonic

The pulse sensor we developed is based on technology in which the behavior of I-Q Lissajous output by the radio wave sensor is analyzed to estimate the movement on the body surface. For this, we prepared an analysis tool which enables the observation of I-Q Lissajous as shown in Fig. 6 for development. For the evaluation criterion, an ear-clip type pulse sensor which can detect volume pulse waves is separately used as a reference sensor. Hereinafter, the pulse rate value estimated by using a microwave Doppler sensor is referred to as the "MDS value" and the pulse rate value estimated by using a reference sensor is referred to as "Reference (Ref.) value". The pulse rate estimate accuracy is shown by evaluating the RMS (Root Mean Square) error between the MDS value and reference value.
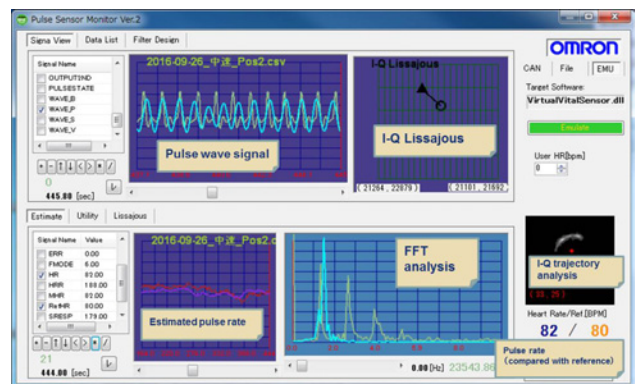

Fig. 6 Pulse sensor output analysis tool

4.1 Estimation of the offset of I-Q Lissajous

Since the pulse rate is estimated by analyzing the behavior of I-Q Lissajous, the I-Q offset coordinate which becomes the center of the circular path of I-Q Lissajous (I_{offset} and Q_{offset}) significantly influences the estimate accuracy of the pulse rate. Therefore, we developed technology for estimating the I-Q offset from the trajectory of the I-Q signal. The I-Q offset varies greatly when there is a change in the positional relationship between the pulse sensor and a peripheral metal object. When installing a pulse sensor in the seat, this technology is essential to ensure accuracy because it is difficult to eliminate peripheral metal objects.
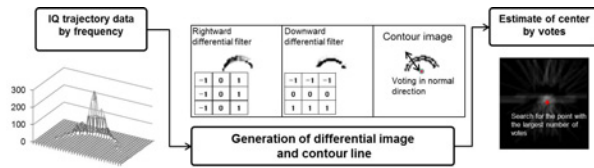

Fig. 7 Estimation of the offset of I-Q Lissajous

As Fig. 7 shows, the trajectory drawn by I-Q Lissajous is observed to accumulate the frequency data which show the passing frequency of each coordinate point.

Differential filter processing is performed for the accumulated frequency data to determine the differential coefficient of each axial direction. Furthermore, the contour line is determined by connecting the points where the initial rise of the frequency data is sharp to create an edge. Based on the respective points that make up this contour line, the normal line direction is determined using the differential coefficient previously obtained to vote for the respective coordinates in the normal line direction. Based on the voting results, the coordinate which gained the largest number of votes is estimated as the center of I-Q Lissajous.

With this method, detecting a change in the measurement environment as a change in the frequency distribution of the trajectory drawn by I-Q Lissajous and correcting the offset position of I-Q Lissajous enabled the building of a radio wave type pulse sensor into a seat where there are many peripheral metal objects.

4.2 Synchronous detection of pulsation

To extract a pulsation signal from being buried in disturbance, we developed our own synchronous detection algorithm. Fig. 8 shows its outline. The signal synchronized with the periodic component of pulsation is extracted as a pulsation signal from the Doppler angular velocity signal that observes the movement on the body surface, and the pulse is detected from the signal to count the pulse number to estimate the pulse rate per minute (bpm). The algorithm we developed provides feedback on the estimated pulse rate to generate a model pulse wave signal

to synchronize with an actual pulsation signal through serial processing. The model pulse wave signal is generated by referring to the table in which the characteristics of the pulse wave with respect to each pulse rate are memorized in advance. The difference between this model pulse wave signal and the pulsation signal after adaptive filter processing is taken, and the coefficient of the adaptive filter is updated so that the mean square of this difference is minimized. Through this operation, the pulsation signal after adaptive filter processing is synchronized with the actual pulsation signal.

The upper part of Fig. 9 shows the raw data before adaptive filter processing and the lower part shows the synchronous detection processing signal after adaptive filter processing. Compared with the signal of the reference sensor, it is determined that the signal after synchronous detection processing is detected in synchronization with the signal of actual pulsation.
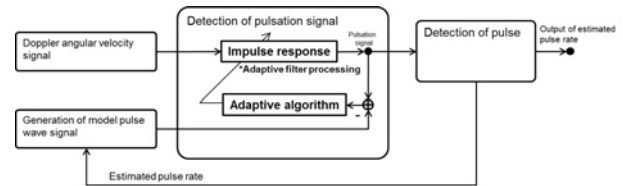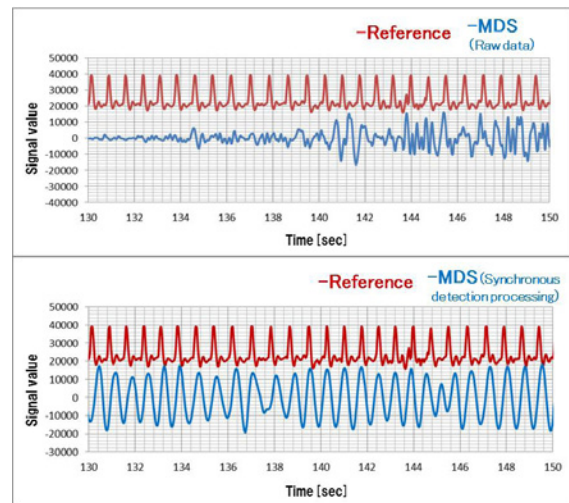

Fig. 8 Synchronous detection algorithm for pulsation

Fig. 9 The effect of synchronous detection processing

4.3 Canceling of respiratory harmonic

Since the algorithm we developed is synchronized with a periodic signal, it could possibly be synchronized with a periodic signal other than pulsation by mistake. Respiratory body movement is a periodic signal on the body surface. Although we assumed that the respiratory body movement could be separated by a bandpass filter because it was lower in frequency than pulsation, since the variation in pulsation is very subtle relative to the variation in respiration and even the harmonic component of the respiratory

period influences the detection of pulsation significantly, it is necessary to control this respiratory harmonic component.

Fig. 10 shows the outline of the algorithm which cancels the respiratory harmonic. As is the case with the synchronous detection method, the processing is configured by an adaptive filter. Respiratory components are extracted from the Doppler angular velocity signal to estimate its harmonic. The respiratory harmonic is passed through the adaptive filter, the difference between it and the Doppler angular velocity signal is taken, and the coefficient of the adaptive filter is updated so that the mean square of this difference is minimized. In addition, the signal from which the difference was taken is output as the signal which canceled the respiratory harmonic. Since the respiratory harmonic component is suppressed in the Doppler angular velocity signal through this operation, accidental synchronization with the respiratory harmonic can be prevented.

Fig. 11 shows the case where the efficacy was confirmed through frequency analysis. The upper part of Fig. 11 shows the relationship between the pulsation period and respiratory component period based on a comparison with the reference signal. Since bandpass filter processing was performed in advance, the size of the respiratory component is small. The pulsation component of the Doppler angle rate signal is sandwiched between the respiratory harmonic components, showing the situation where it is difficult to synchronize with the pulsation component.

The lower part of Fig. 11 shows the analysis results after cancelling the respiratory harmonic. The improved situation where the respiratory harmonic components are suppressed and it is easy to synchronize with the pulsation component is shown.
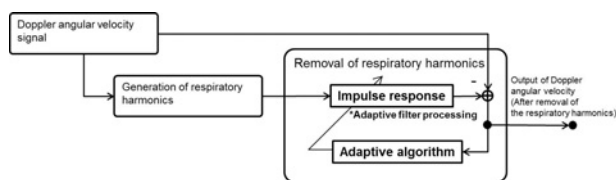
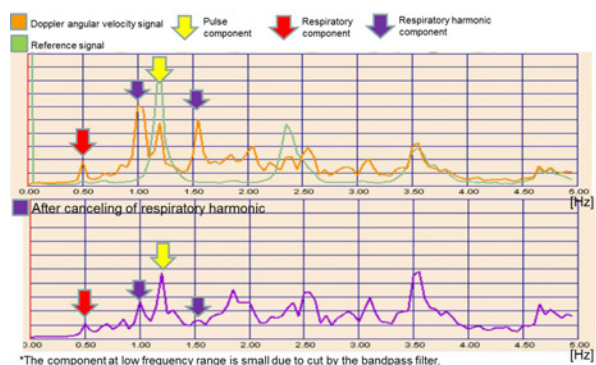

Fig. 10 Canceling of respiratory harmonic

Fig. 11 The efficacy of the canceling of respiratory harmonic through frequency analysis

5. Performance evaluation

The aforementioned technology we independently developed enabled the estimation of the pulse rate with high accuracy even while running.
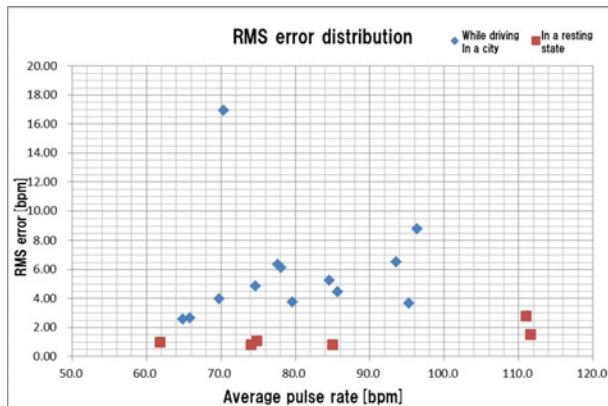

Fig. 12 RMS error distribution of estimated pulse rates

Fig. 12 shows the RMS error distribution of the estimated pulse rates of six drivers in a resting state and thirteen drivers driving in a city.

In the case of the drivers in a resting state, the RMS error was 5 bpm or lower. In the case of the drivers driving in a city, it was approximately 10 bpm or lower. Among the thirteen drivers driving in a city, one driver experienced an RMS error far exceeding 10 bpm. This is estimated to have been caused by improper measurement, because the body surface of the measurement site is compressed depending on the seating position and it was difficult to detect the pulsation component. To realize an environment where the measurement can be performed more stably, it is important to improve the method of installing the pulse sensor in the seat.

Fig. 13 shows the data of three drivers who were in a resting state, which were measured in comparison with the reference sensor for two minutes. When the drivers were in a resting state, the measurement results relatively coincided with the reference value.

Fig. 14 shows the data of twenty-minute drive in a city performed by three drivers as a result of measurement in comparison with the reference sensor. Although the errors increased owing to the disturbance while driving, the measurement results coincided with the reference value on average.

Although it is still necessary to make improvements to enable stable measurement in any seating position by adjusting the pulse sensor installation conditions, it can be said that we almost achieved the development goal concerning the performance of the pulse sensor alone.
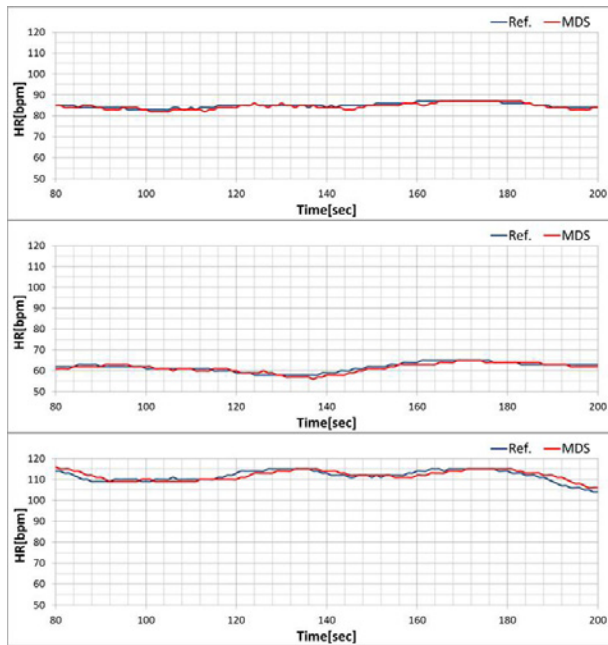
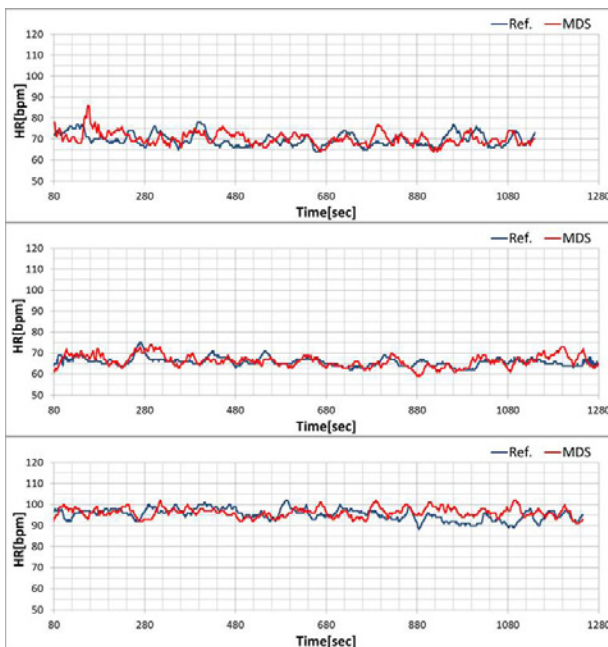**Fig. 13** Estimate accuracy of pulse rate in a resting state

Fig. 14 Estimate accuracy of pulse rate while driving in a city

6. Conclusion

One of the major purposes is to enlighten drivers about the importance of health control by notifying them of the results of measuring the pulse rate while driving using an in-vehicle pulse sensor. In particular, driving is a physically and mentally taxing task, and there is a strong tendency for the pulse rate to become higher than in the normal state. It is generally said that the risk of heart disease increases if the pulse rate becomes high. To prevent accidents attributable to health, it is important to care for one's health on a regular basis to avoid the onset of illness

while driving. Drivers whose pulse rates tend to increase while driving need to be encouraged to drive in a healthier state by reconsidering their daily habits.

The pulse sensor we developed this time enables the measurement of the pulse rate without bothering drivers, as it is built into the seat. On the other hand, there are cases where the measurement cannot be performed properly if the body surface of the measurement site is compressed depending on the seating position. In addition, in the event of significant disturbance, it is difficult to follow the rapid variation in the pulse rate and initial stabilization time for synchronous detection is required. Therefore, the responsiveness and stability needs to be enhanced further to respond to more advanced applications such as the eCall system utilizing the variation in pulse rate and emotion estimation. In the future, we will evolve the performance of the pulse sensor further to work toward resolving social issues.

References

1) A. Mase:Biological Measurement by Using Microwave Active Sensor and Applications, JOURNAL OF THE SOCIETY OF INSTRUMENT AND CONTROL ENGINEERS 3 VOL.50, 2011, p.233.

About the Authors

MITANI Shigetomo

Technology Development Department
OMRON AUTOMOTIVE ELECTRONICS Co.,Ltd.
Specialty: Mechanical system engineering
Affiliated Academic Society: SICE

The names of products in the text may be trademarks of each company.